

Sensitivity studies in the search for anomalous quartic gauge couplings in proton-proton collisions

*Claire Yang
youyou.yang@mail.mcgill.ca

June 30, 2024

Abstract

New physics can be built from the frame of Standard Model Effective Field Theory(SMEFT), but with unknown coefficients of operators in the theory. The anomalous quartic gauge coupling(aQGC) is one of them. To increase the completion of the theory, we start from the Vector boson scattering (VBS) $W\gamma$ reaction data to set constraints on the coupling coefficient, which requires finding operators and kinematic variables which are sensitive to aQGC. We ended up with the conclusion that the T-type operator would be more sensitive to the VBS $W\gamma$ reaction than the M-type, especially O_{T6} . The selected sensitive variables are di-jet p_T , E_γ , lepton p_T and $m_{W\gamma}$. Unfortunately, almost all variables we analyzed to date were less sensitive to small values of aQGC. Our next step could be quantifying the VBS cross-section of the sensitive kinematic variables to help set constraints on the aQGC operators.

1 Introduction

1.1 Effective Field Theory of the Standard Model

Interactions between gauge bosons (W boson, Z boson, and photon) are predicted by the Standard Model of particle physics. New physics beyond the Standard Model can be built from deviations from the prediction. In this case, Effective Field Theory (EFT) is a powerful tool. It contains the degrees of freedom and parameters needed to describe phenomena at a given scale Λ . So it is restricted to a scope above a length scale, or saying, below an energy scale. Thus it is independent of the Standard Model. According to the above assumptions of EFT, the low energy effect that is beyond the kinematics of the experiment can not be observed directly, but the deviation from prediction can be detected. These effects are achieved by introducing a new set of higher-dimension operators. Thus an EFT can be derived by the combination of higher dimension operators and the Standard Model Lagrangian.

$$\mathcal{L}_{EFT} = \mathcal{L}_{SM} + \sum_{n=5}^{\infty} \frac{\tilde{f}_n}{\Lambda^{n-4}} \mathcal{O}_i \quad (1)$$

Here the Standard Model Lagrangian \mathcal{L}_{SM} dimension below 4 is counted as effective, so the operator term starts from dimension $n = 5$. The coefficient $\tilde{f}_n/\Lambda^{n-4}$ represents the effective coupling strength of operator \mathcal{O}_i , which is unknown for so far. So we have a motivation to work on the new physics to establish a narrower range for the coupling strength.

Treat equation (1) as a combination of matrices and square it:

$$|A_{SM} + c_i A_{O_i}|^2 = A_{SM}^2 + c_i A_{SM} A_{O_i} + c_i^2 A_{O_i}^2. \quad (2)$$

The coefficient c_i equals to the coupling strength $\tilde{f}_n/\Lambda^{n-4}$. From this equation, the EFT of the aQGC can be split into three terms: the contribution of the Standard Model only, the contribution of the operator only (quadratic term), and the contribution of the interference between the EFT and the Standard Model (linear term).

*Supervised by Brigitte Vachon, John McGowan and Xingguo Li

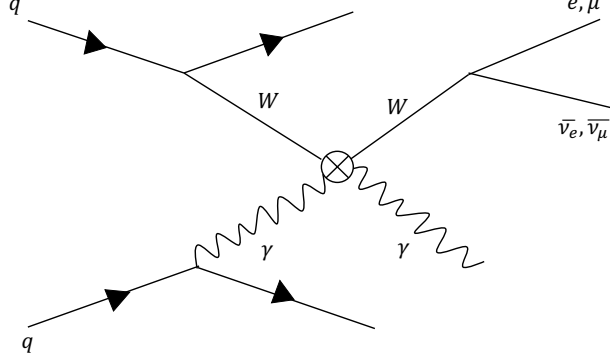


Figure 1: Feynman diagram of the $WW\gamma\gamma$ vertex.[4]
 q stands for quark, W for W boson, γ for photon, e, μ are the leptons, $\bar{\nu}$ for neutrino.

Table 1: Dimension-8 operators and the quartic vertices they affect. [5]

	WWWW	WWZZ	WW γ Z	WW $\gamma\gamma$	ZZZZ	ZZZ γ	ZZ $\gamma\gamma$	Z $\gamma\gamma\gamma$	$\gamma\gamma\gamma\gamma$
$O_{S,0}, O_{S,1}$	✓	✓			✓				
$O_{M,0}, O_{M,1}, O_{M,6}, O_{M,7}$	✓	✓	✓	✓	✓	✓	✓		
$O_{M,2}, O_{M,3}, O_{M,4}, O_{M,5}$		✓	✓	✓	✓	✓	✓		
$O_{T,0}, O_{T,1}, O_{T,2}$	✓	✓	✓	✓	✓	✓	✓	✓	✓
$O_{T,5}, O_{T,6}, O_{T,7}$		✓	✓	✓	✓	✓	✓	✓	✓
$O_{T,8}, O_{T,9}$					✓	✓	✓	✓	✓

1.2 The $WW\gamma\gamma$ vertex and its corresponding operators

One of the new physics that can arise from the Standard Model is the triple or quartic gauge boson coupling[3]. Vector boson scattering (VBS), also referred to as electroweak gauge boson scattering, is the process that can be realized by anomalous quartic gauge coupling (aQGC). In this study, we mainly focus on the $WW\gamma\gamma$ coupling as in fig. 1, which is one of the possible VBS reactions. To set a more precise range for the coupling strength, we aim to have more data on the reaction. Thus the sensitive kinematic variables needed to be selected to put into the function, so that the sensitivity of the data can be maximized. Also, the sensitivity of the operator needs to be taken into account, such that the scope of coupling strength can be better established for this aQGC.

Quartic gauge boson coupling is directly sensitive to the effects of Dimension-8 operators (see table 1). According to the table, the M-type operators and T-type operators contribute to our $WW\gamma\gamma$ vertex.

1.3 Existing constrains on the operators

Although the anomalous gauge coupling does not have an exact value for coupling strength yet, a wide range of constraints already exists from the Large Hadron Collider (LHC). According to the figure 2, the rough constrain value for M-type operators are of order $O(1 - 100 \text{ TeV}^{-4})$ and $O(0.1 - 10 \text{ TeV}^{-4})$ for T-type[1].

2 Data

In this study, we used data at the reconstructed level after simulation to acquire the most possible data. The simulated signal of the VBS $W\gamma$ vertex is generated with the EFT model by MadGraph[2]. Events for the linear term and quadratic in 2 is generated individually. The default coupling value of all the operators in the simulation of the data is 2.4 TeV^{-4} .

We directly plotted the reconstructed raw data of all kinematic variables of all operators in the form of histograms. We applied $(1, 10, 100 \text{ TeV}^{-4})$ as the coupling value of the M-type operator, and $O(0.1, 1, 10 \text{ TeV}^{-4})$ for T-type operator. Then the histograms including operators with three coupling values are shown, as well as the percentages of deviation between the histogram with respect to the prediction of the Standard Model. Figure 6 using O_{M2} data in appendix can be referred as a example of the partial data. Comparing the size of

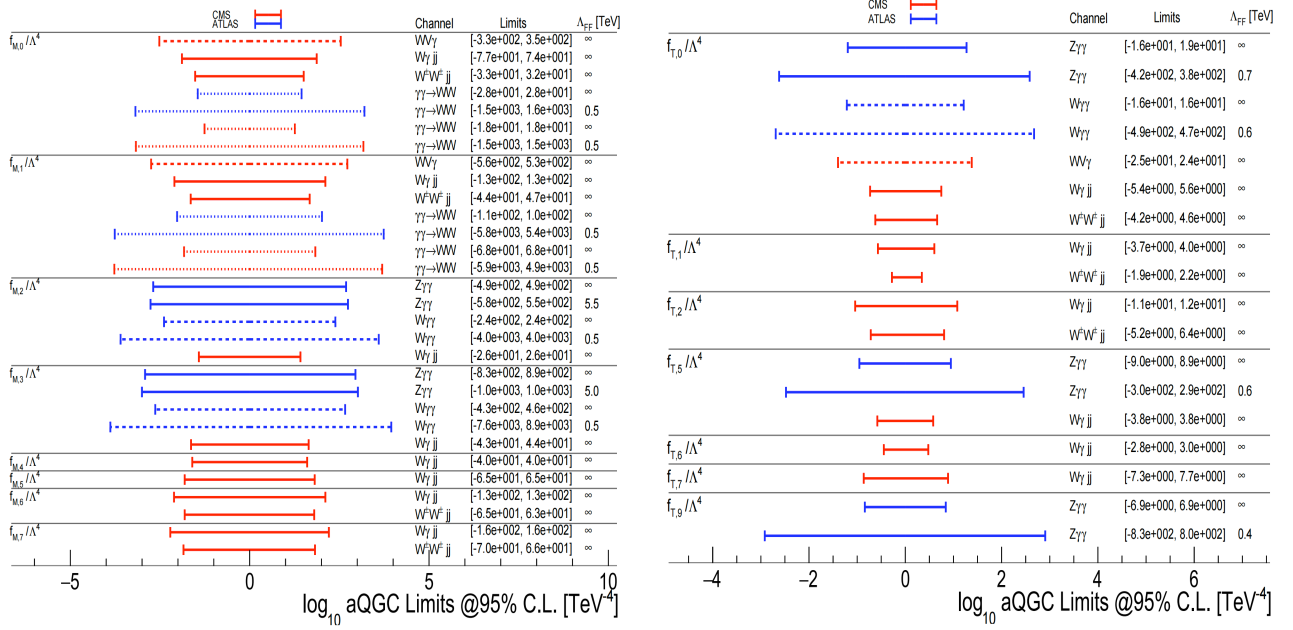


Figure 2: Existing constraints on "M" and "T" types Dimension-8 operators from LHC.

the deviation and the changes in shapes of the histograms, we concluded a roughly more sensitive collection of variables, which for further analysis we focused on:

E_γ , $p_{T,lepton}$, $p_{T,leading\ jet}$, $p_{T,second\ leading\ jet}$, $m_{W\gamma}$, and signed $\Delta\Phi_{lepton\gamma}$,

where E means the energy, p_T means the transverse momentum, m means the invariant mass, and Φ means the flat angle around the bin.

Besides the collection of variables we just selected, the di-jet variables m_{jj} , $p_{T,jj}$, $\Delta\phi_{jj}$ were also taken into account in the study. As they have been recognized to be valuable for the differential cross-section function of the VBS reaction, which will help to set constrain on the aQGC operators.

In order to put us in a phase space where the events are dominated by the particular $WW\gamma\gamma$ reaction as in figure 1, We applied the following pre-selection to the data:

- Lepton (e, μ) satisfy baseline pre-selection cuts
- $m_{jj} > 1000 GeV/C^2$
- $|\Delta y_{jj}| > 2 rad$
- $centrality_{W\gamma} < 0.35$.

As our $WW\gamma\gamma$ reaction is at high m_{jj} , low centrality, and high rapidity difference (Δy_{jj}).

3 Analysis

3.1 Sensitivity to different types of operators

We superimposed all the M-type and T-type operators separately and looked to find which operator resulted in the largest deviations from the Standard Model expectations. The coupling strength of all Dimension-8 operators considered was set to $\tilde{f}_n/\Lambda^{n-4} = 1\ TeV^{-4}$. We only plotted the operators on the variables chosen above with the raw data. The plot for variable $E_\gamma, p_{T,lepton}, and m_{W\gamma}$ is shown in figure 3, whose shaping very representative and are all in agreement with our final conclusion.

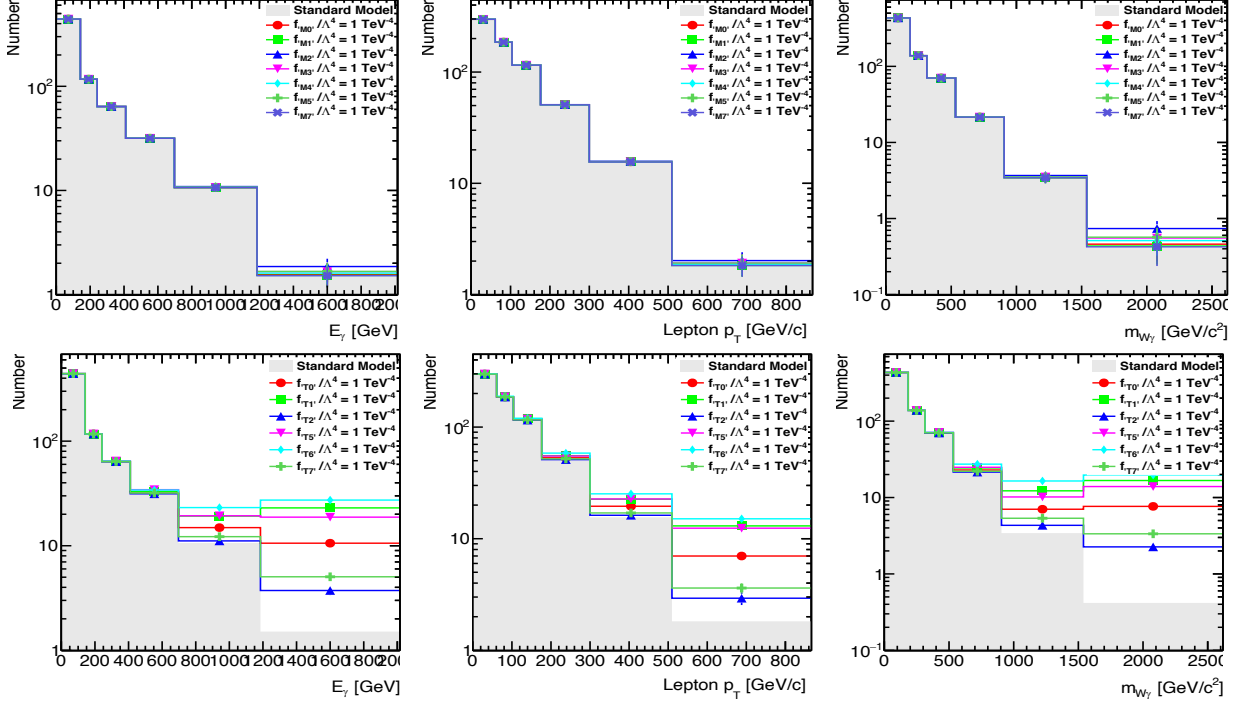


Figure 3: Sensitivity comparison of E_γ , $p_{T,lepton}$, and $m_{W\gamma}$ to all M and T type operators contributing to the $WW\gamma\gamma$ vertex, with a coupling strength $\tilde{f}_n/\Lambda^{n-4} = 1 \text{ TeV}^{-4}$.

It is obvious that the histograms of the T-type operators are far from the prediction of the Standard Model, unlike the M-type operators are very close. Therefore, the sensitivity of T-type operators is higher than that of M-type to the reaction.

For all T-type operators, the largest deviation appears for O_{T6} . Hence the strongest sensitive operator is O_{T6} , followed by O_{T1} , O_{T5} , O_{T0} , O_{T7} , and O_{T2} . While for the M-type operator, O_{M2} deviates the most, so it takes the most sensitivity to the VBS $W\gamma$ reaction, and followed by O_{M5} and O_{M3} .

3.2 Sensitivity to different kinematic variables

The variables chosen in section 2 were plotted applying the coupling value $\{1, 10\} \text{ TeV}^{-4}$ for M-type operator, and $\{0.1, 1\} \text{ TeV}^{-4}$ for T-type operator. The histograms are then plotted in the same approach as the raw data, except that we have streamlined the binning to be more precise and selective. Since we already have some knowledge about the di-jet variables, the following agreed-upon binning is used:

- $p_{T,jj}$: 0, 55, 80, 125, 180, 270, 840.
- m_{jj} : 1000, 1450, 1800, 2300, 5300.
- $\Delta\phi_{jj}$: -3.1416, -2.9452, -2.7489, -2.4435, 0., 2.4435, 2.7489, 2.9452, 3.1416.

For other kinematic variables, divided distributions in approximately 5-10 bins to represent the approximate granularity at which a differential cross-section could be made.

Figure 4 show an example of expected distributions from O_{T6} , but the conclusion is the same for other operators. Comparing the deviations from the Standard Model to the prediction with the existence of the operators, we identified the following variables to be sensitive to aQGC: di-jet p_T , E_γ , lepton p_T and $m_{W\gamma}$.

However the kinematic variable $m_{W\gamma}$ is considered to be correlated to E_γ and lepton p_T . So there might be a preferred choice to simplify the last three variables we have just chosen to only the $m_{W\gamma}$ or a combination of E_γ and lepton p_T .

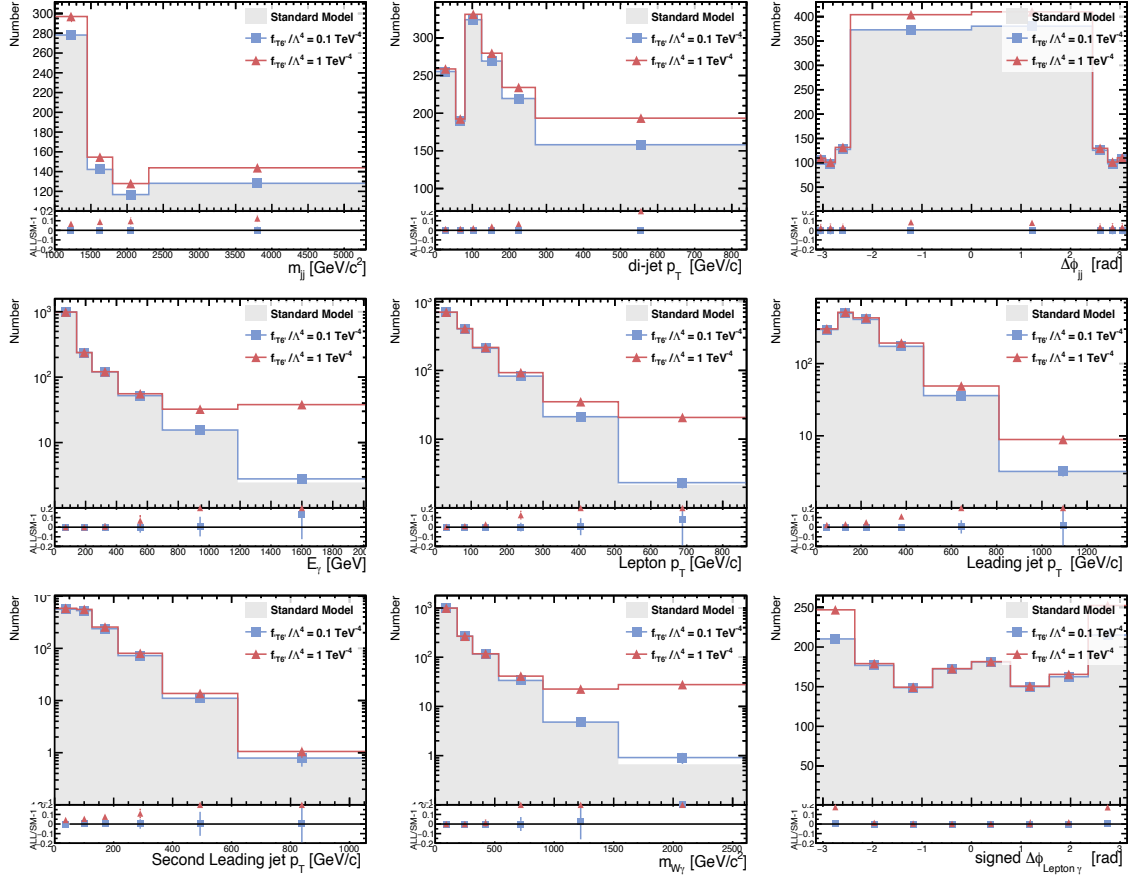


Figure 4: Distributions for different kinematic variables of T6 operator.

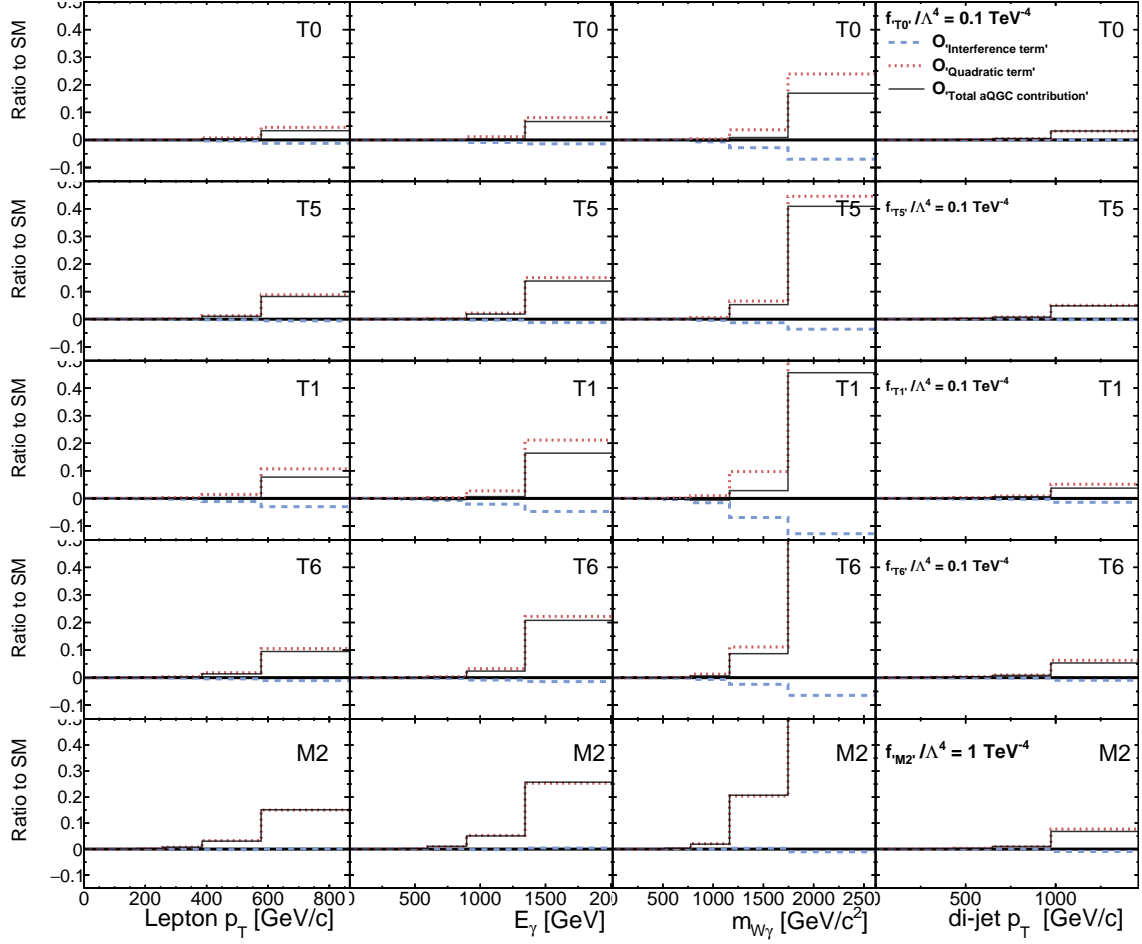


Figure 5: The ratio with respect to SM for interference term and quadratic term separately for $O_{T0}, O_{T5}, O_{T1}, O_{T6}, O_{M2}$ for the sensitive variables.

3.3 Further selection

We also want to identify variables most sensitive to small values of aQGC, which means coupling constraints obtained from variables most sensitive to (linear) interference term considered more robust to extrapolation. To achieve that, smallest coupling value are chosen for each operator, which is $\{1, 10\} \text{TeV}^{-4}$ for M-type operator, and $\{0.1, 1\} \text{TeV}^{-4}$ for T-type operator. Then we plotted the ratio with respect to SM for the interference and quadratic term separately for the operators and kinematic variables we just selected.

As seen from the results in figure 5, the interference term is not only more minor in absolute value than the quadratic term, but also appears to have a negative ratio mostly. So we came to the conclusion that for the variables we just selected to be sensitive, their sensitivity to aQGC is dominated by the quadratic term.

To enhance the generality of the conclusions as well as to detect variables sensitive to small values of aQGC, we repeated the above steps with the relatively less sensitive di-jet and angular variables in figure 7. Although the difference between the absolute ratio of the two terms became smaller than before, the conclusions remained unchanged.

4 Conclusion

We have studied the sensitivity of a vector boson scattering reaction to the presence of anomalous quartic gauge couplings. For comparing the operators, the T-type operators are much more sensitive to VBS $W\gamma$ reaction than the M-type operators when the constraint is consistent. Among all the operators the most sensitive is O_{T6} , also the $O_{T1}, O_{T5}, O_{T0}, O_{M2}$ shows some sensitivity to the aQGC. (listed in order of sensitivity) For the kinematic variables most sensitive to aQGCs are: E_γ , lepton p_T and $m_{W\gamma}$. The three di-jet variables $m_{jj}, p_{T,jj}, \Delta\phi_{jj}$

should also be taken into account due to the previous study. All kinematic variables investigated to date show sensitivity to aQGC dominated by the pure dimension-8 (quadratic) term.

Our next step can be to implement an analysis framework to set constraints on aQGCs based on the measurement of the VBS cross-section as a function of the kinematic variables identified above.

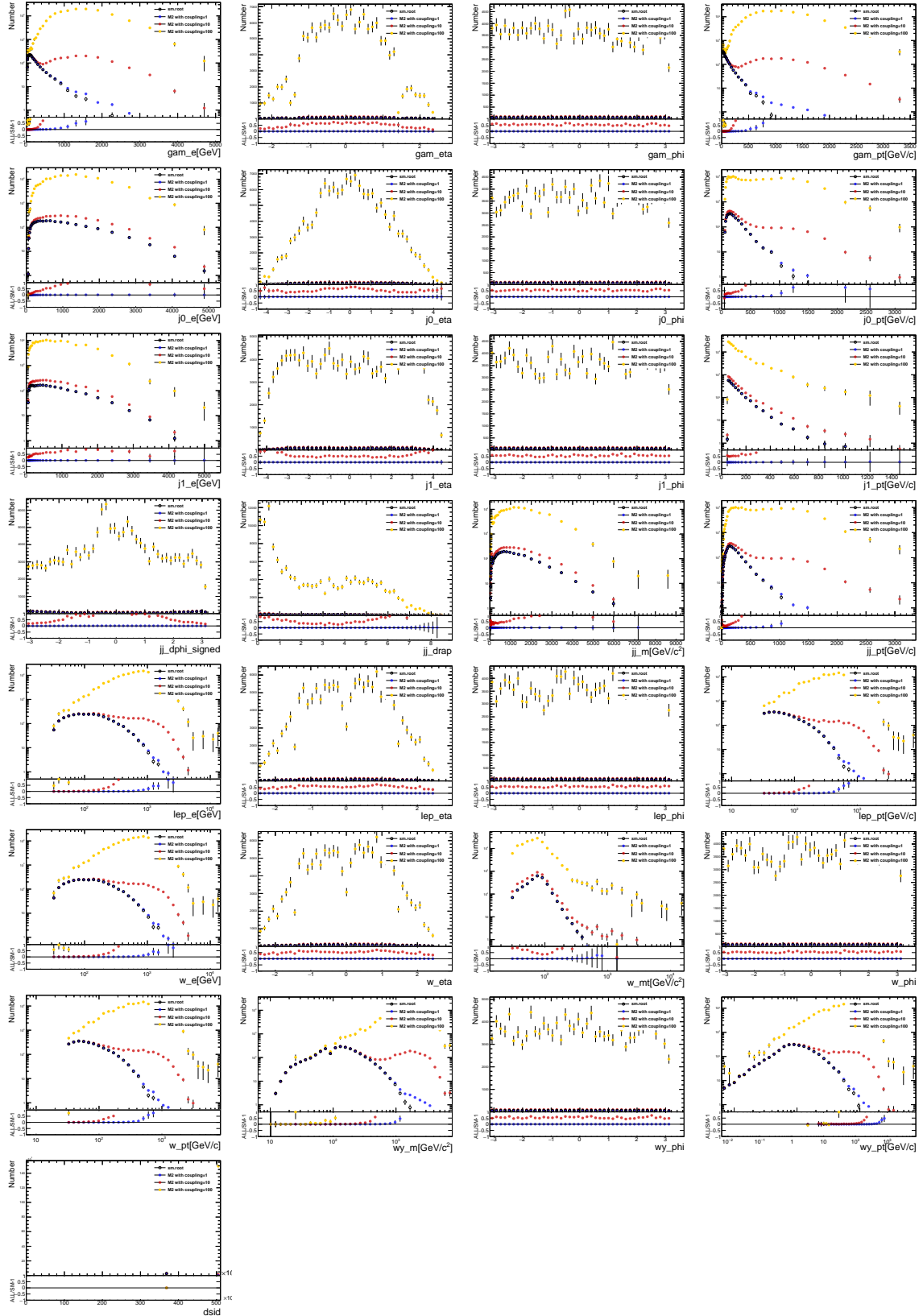
References

- [1] Limits on anomalous triple and quartic gauge couplings, 2020.
- [2] Johan Alwall, Michel Herquet, Fabio Maltoni, Olivier Mattelaer, and Tim Stelzer. MadGraph 5: going beyond. *Journal of High Energy Physics*, 2011(6), jun 2011.
- [3] P J Dervan, A Signer, W J Stirling, and A Werthenbach. Anomalous triple and quartic gauge boson couplings. *Journal of Physics G: Nuclear and Particle Physics*, 26(5):607–615, apr 2000.
- [4] Raquel Gomez-Ambrosio. Vector Boson Scattering Studies in CMS: The $pp \rightarrow ZZjj$ Channel. *Acta Phys. Pol. B Proc. Suppl.*, 11:239–248. 10 p, Jul 2018.
- [5] D. R. Green, P. Meade, and M.-A. Pleier. Multiboson interactions at the LHC. *Reviews of Modern Physics*, 89(3), sep 2017.

A Acknowledgment

Special thanks to Brigitte Vachon, John McGowan and Xingguo Li.

B Additional figures



1

Figure 6: Raw data of M2 operator.

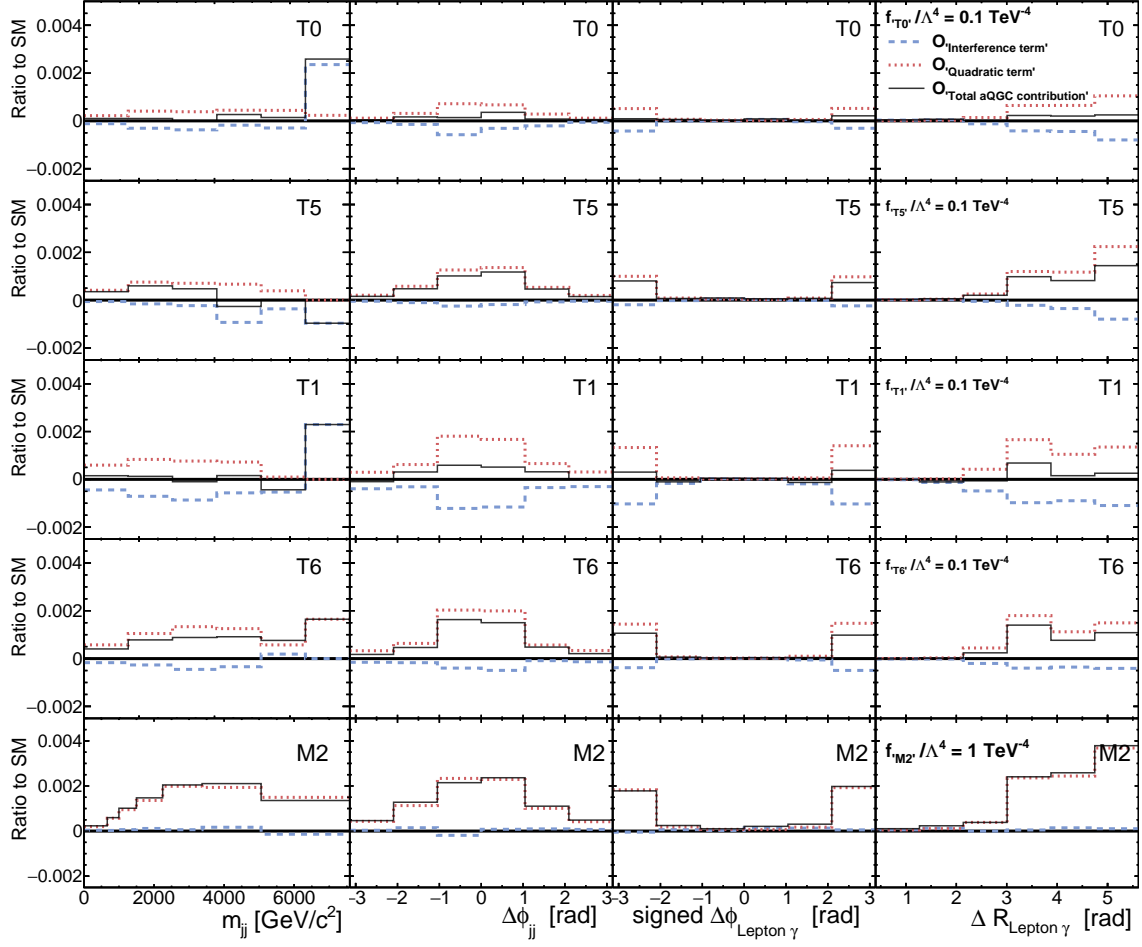


Figure 7: The ratio with respect to SM for interference term and quadratic term separately for $O_{T0}, O_{T5}, O_{T1}, O_{T6}, O_{M2}$ for the di-jet and angular variables.